Title
Nitrogenase and homologs.

Journal
Journal of biological inorganic chemistry : JBIC : a publication of the Society of Biological Inorganic Chemistry, 20(2)

ISSN
0949-8257

Authors
Hu, Yilin
Ribbe, Markus W

Publication Date
2015-03-01

DOI
10.1007/s00775-014-1225-3

Peer reviewed

Published in final edited form as:
J Biol Inorg Chem. 2015 March ; 20(2): 435–445. doi:10.1007/s00775-014-1225-3.

Nitrogenase and Homologs

Yilin Hu and
Department of Molecular Biology and Biochemistry, 2230 McGaugh Hall, University of California, Irvine, CA 92697-3900

Markus W. Ribbe
Department of Molecular Biology and Biochemistry, 2236 McGaugh Hall, University of California, Irvine, CA 92697-3900; Department of Chemistry, University of California, Irvine, California 92697-2025

Yilin Hu: yilinh@uci.edu; Markus W. Ribbe: mribbe@uci.edu

Abstract

Nitrogenase catalyzes biological nitrogen fixation, a key step in the global nitrogen cycle. Three homologous nitrogenases have been identified to date, along with several structural and/or functional homologs of this enzyme that are involved in nitrogenase assembly, bacteriochlorophyll biosynthesis and methanogenic process, respectively. In this article, we provide an overview of the structures and functions of nitrogenase and its homologs, which highlights the similarity and disparity of this uniquely versatile group of enzymes.

Keywords

Nitrogenase; CO/CO_2 reduction; radical SAM; interstitial carbide; homolog; bacteriochlorophyll biosynthesis; methanogenesis

Nitrogenases are a family of complex metalloenzymes that catalyze the reduction of nitrogen (N_2) to ammonia (NH_3) under ambient conditions [1–4]. Three homologous nitrogenases have been identified to date, which contain cofactors that are mainly distinguishable by the heterometals they contain at their respective cofactor sites: the "conventional" molybdenum-containing nitrogenase, the "alternative" vanadium-containing nitrogenase, and the "alternative" iron-only nitrogenase [2, 5]. Apart from these homologous forms of nitrogenases, several structural/functional homologs to nitrogenases have been identified in recent years, including proteins involved in nitrogenase assembly, bacteriochlorophyll biosynthesis and methanogenic process [6, 7]. Here, we provide an overview of the structures and functions of nitrogenases and homologs, which highlights the similarity and disparity of this uniquely diversified "super family" of enzymes.

Correspondence to: Yilin Hu, yilinh@uci.edu; Markus W. Ribbe, mribbe@uci.edu.

The Molybdenum (Mo) Nitrogenase

The Mo nitrogenase, which has been isolated from *Azotobacter vinelandii*, *Klebsiella pneumoniae* and *Clostridium pasteurianum* [8–10], is undoubtedly the best characterized member of this enzyme family. It consists of two separately purifiable, oxygen-sensitive, metallosulfur proteins, which are designated the iron (Fe) protein and the molybdenum-iron (MoFe) protein, respectively [1]. The Fe protein belongs to a family of nucleotide-utilizing proteins [1, 8], and it serves as an ATP-dependent reductase in nitrogenase catalysis. Encoded by *nifH*, the Fe protein is a homodimer of *Mr* ~ 60 kDa. The primary sequence of the Fe protein has a GXGXXG consensus motif, which provides a binding site for MgATP in each subunit of this homodimeric protein. Moreover, the two subunits of this protein are bridged by a [Fe_4S_4] cluster (Fig. 1A and B) through four Cys residues, two from each subunit [11]. The MoFe protein is the catalytic partner of the Fe protein in nitrogenase catalysis. It is an $\alpha_2\beta_2$-tetramer of *Mr* ~ 220 kDa, and its α- and β-subunits are encoded by *nifD* and *nifK*, respectively [8, 9, 11]. The MoFe protein contains two unique metallosulfur clusters (Fig. 1A and B): the P-cluster ([Fe_8S_7]), which is bridged between each $\alpha\beta$-subunit pair by six Cys residues; and the FeMo cofactor, or the M-cluster ([$MoFe_7S_9C$-homocitrate]), which is located within each α-subunit and coordinated by a His residue and a Cys residue at the opposite ends of the cluster [3, 11].

The x-ray crystal structures of both component proteins of the Mo nitrogenase have been resolved [12–17] and, while the structure of the MgATP-bound form of the Fe protein is unknown, the small angle x-ray scattering (SAXS) data have shown that the conformational change of the Fe protein upon MgATP binding/hydrolysis causes a contraction of the protein by 2.0 Å on average [18]. It has been proposed, therefore, that the conformational rearrangement of the Fe protein upon ATP binding/hydrolysis allows it to dock on the MoFe protein, which then facilitates the inter-protein electron transfer from the Fe protein to the MoFe protein and the reduction of substrates at the M-cluster of the MoFe protein. Consistent with this hypothesis, the x-ray crystallographic analysis of a MgADP·AlF_4^--stabilized complex between the Fe protein and the MoFe protein [15], which represents the "transition state" during MgATP hydrolysis, provides some compelling evidence that the electrons are transferred sequentially from the [Fe_4S_4] cluster of the Fe protein, via the P-cluster, to the M-cluster of the MoFe protein (Fig. 1A and B). Substrate reduction is believed to take place once the M-cluster accumulates a sufficient amount of electrons, followed by the release of the products, the dissociation of the complex between the Fe protein and the MoFe protein, and the initiation of a new round of substrate reduction.

The overall reaction catalyzed by the Mo nitrogenase is usually depicted as follows: $N_2 + 8H^+ + 16MgATP + 8e^- \rightarrow 2NH_3 + H_2 + 16MgADP + 16P_i$ [19]. Other than its physiological substrates [*i.e.*, N_2 and proton (H^+)], the Mo nitrogenase is also capable of reducing a wide range of small doubly- and triply-bonded substrates, such as acetylene (C_2H_2), ethylene (C_2H_4), cyanide (CN^-), nitrous oxide (N_2O), nitrite (NO_2^-), azide (N_3^-) and hydrazine (N_2H_4) [1]; in particular, C_2H_2 is an efficient, alternative substrate that has been routinely used for the determination of the enzymatic activities of nitrogenases. Progress was made early on in understanding the interactions between the protein-bound M-cluster and substrates/inhibitors [*e.g.*, C_2H_2, carbon disulfide (CS_2) and carbon monoxide

(CO)], as well as the interactions between the isolated M-cluster and substrates/inhibitors (*e.g.*, CN^- and CO) [20–26]. Recently, CO and carbon dioxide (CO_2) have been either re-classified or defined as substrates for certain Mo nitrogenase variants, as well as substrates for the vanadium nitrogenase (see below), thereby broadening the substrate profile of nitrogenases [27–33]. Further, a combined genetic, biochemical and spectroscopic approach has led to the proposal of the first draft of nitrogenase mechanism, which involves reductive elimination of the M-cluster-bound hydrides (H^-) as hydrogen (H_2) that is obligate for the subsequent activation and reduction of N_2 [34].

One interesting feature of the active site (*i.e.*, the M-cluster) of the Mo nitrogenase is the presence of a μ_6-coordinated light atom in its central cavity. Discovered more than a decade ago [16], this light atom was identified only recently by x-ray emission spectroscopy (XES) and combined high-resolution crystallography/electron nuclear double resonance (ENDOR)/electron spin echo envelope modulation (ESEEM) spectroscopy as a carbide (C^{4-}) ion coordinated by six "equatorial" Fe atoms in the structure of the M-cluster [17, 35]. Biochemical characterization further established the methyl group of *S*-adenosylmethionine (SAM) as the source of the interstitial carbide and suggested a radical-dependent pathway for carbide insertion, which involves hydrogen abstraction of the SAM-derived methyl group by a 5′-deoxyadenosyl radical (5′-dA•) and further processing of the resultant radical carbon intermediate concomitant with radical-based coupling/rearrangement of FeS fragments till a complete Fe/S core of the M-cluster is formed with an interstitial carbide in place [36]. The interstitial carbide is not exchangeable upon turnover with N_2, C_2H_2 and CO, which points to a structural function of this atom in stabilizing the active center of Mo nitrogenase [37]. Nevertheless, an indirect role of this atom in regulating the reactivity of the M-cluster cannot be excluded, particularly in light of a study describing the activation of N_2 on iron metallaboratranes, which suggests that the interstitial atom may allow variation of the Fe-C bond distances and modulation of the metal-sulfur core geometry during catalysis [38]. Moreover, the recent observation of non-CO_2-based methane (CH_4) formation by Mo nitrogenase in the presence of CO_2 suggests the interstitial carbide as one potential source for CH_4 formation in this case, which may originate from the interaction between CO_2 and the interstitial carbide and the subsequent release of this atom in the form of CH_4 [27].

The Vanadium (V) Nitrogenase

Although the role of V in enhancing nitrogen fixation by diazotrophic microorganisms was documented as early as that of Mo [39], the existence of an "alternative", V-containing form of nitrogenase was only verified in the late 1980s, when this enzyme was purified from the tungsten (W)-tolerant mutants of *A. chroococcum* [40–42] and *A. vinelandii* [43–45] in which the structural genes of Mo nitrogenase were deleted. Like its Mo counterpart, the V nitrogenase is also a two-component enzyme system consisting of the Fe protein and the vanadium-iron (VFe) protein [2, 5]. Moreover, the two nitrogenases share a good degree of homology in the primary sequences and the cluster compositions of their component proteins. For example, the *vnfH*-encoded Fe protein (also designated VnfH) in the V nitrogenase, which is a homodimer of *Mr* ~ 60 kDa, has the same subunit composition and molecular mass as its *nifH*-encoded counterpart (also designated NifH) in the Mo nitrogenase. It shares 91% sequence identity with its *nifH*-encoded counterpart [5], and it

also has the same, conserved Cys ligands for the subunit-bridging [Fe_4S_4] cluster, as well as the GXGXXG consensus nucleotide-binding motif, in its primary sequence. Likewise, despite the presence of an extra *vnfG*-encoded δ-subunit, the *vnfD*- and *vnfK*-encoded α- and β-subunits of the VFe protein share ~33% and ~32% sequence identity, respectively, with the *nifD*- and *nifK*-encoded α- and β-subunits of the MoFe protein [5], and the ligands for both the P- and M-clusters in the MoFe protein are also conserved in the sequence of VFe protein. The subunit composition of VFe protein, however, seems to vary between organisms, with the VFe protein purified from *A. chroococcum* being an $\alpha_2\beta_2\delta_2$-hexamer of *Mr* ~ 240 kDa [2] and the VFe protein purified from *A. vinelandii* being an $\alpha_2\beta_2\delta_4$-octamer of *Mr* ~ 270 kDa [46].

Consistent with the presence of the same cluster ligands as those in the Mo nitrogenase, the V nitrogenase contains a set of metal centers that are highly homologous to those in its Mo counterpart; yet, these clusters also display structural/redox features that are clearly distinct from those in the Mo nitrogenase. For example, the *nifH*- and *vnfH*-encoded Fe proteins are believed to contain identical [Fe_4S_4] clusters; however, a recent XAS/EXAFS investigation revealed a less ferric nature of the Fe atoms in the cluster of the *vnfH*-encoded Fe protein than those in the cluster of the *nifH*-encoded Fe protein. Moreover, this study demonstrated that the [Fe_4S_4] cluster in the *vnfH*-encoded Fe protein was best modeled by two stacked [Fe_2S_2] rhomboids offset by 90 degrees; whereas the cluster in the *nifH*-encoded Fe protein could also be modeled by two unequal [Fe_2S_2] rhomboids bent to a greater degree out-of-plane [47]. Likewise, the P-cluster of the VFe protein has long been regarded equivalent to its counterpart in the MoFe protein [48, 49]. However, a more recent electron paramagnetic resonance (EPR) investigation indicated that the P-cluster in the VFe protein existed in a more oxidized state than its counterpart in the MoFe protein in the resting state. Additionally, XAS/EXAFS analysis of the cofactor-deficient VFe protein [5, 50] supplied further proof for the presence of a different P-cluster in the VFe protein, suggesting that this P-cluster (designated the P*-cluster) may consist of paired [Fe_4S_4]-like clusters instead of the usual [Fe_8S_7] structure (Fig. 2)[1]. Finally, the FeV cofactor, or the V-cluster, of the VFe protein has also been shown to be highly similar to the M-cluster of MoFe protein [43, 48, 51–54]. However, the EPR features of the two cofactors are clearly distinct from each other, suggesting a difference between the electronic properties of the two cofactors, as well as the interactions between the cofactors and their respective host proteins [46]. Consistent with the observed spectral differences, XAS/EXAFS analysis of the *N*-methylformamide (NMF)-extracted cofactors [55] revealed that despite a close resemblance between their metal-sulfur core structures, the isolated V-cluster was of a more octahedral symmetry, whereas the isolated M-cluster was of a tetrahedral/trigonal pyramidal structure (Fig. 2). Together, these

[1]The heterogeneity of earlier VFe protein preparations, likely resulting in a mixture of different cluster species, has hampered a thorough investigation of the physiochemical properties of this protein for a long time. Taking advantage of a fast, affinity chromatography-based purification procedure, a His-tagged VFe protein was later purified from *A. vinelandii* as a homogeneous species with high specific activity [46]. In these homogeneous protein preparations, the P-cluster-associated $S = 1/2$ signal, which was previously assigned to an inactive protein species, displays a clear correlation to the specific activity of the proteins, suggesting that this P-cluster species (designated the P*-cluster) is associated with an active form of the protein. An identical $S = 1/2$ signal is also present in a cofactor-deplete, yet P-cluster-replete form of VFe protein, further establishing the P*-cluster as the origin of this $S = 1/2$ signal. Moreover, the Fe K-edge XAS/EXAFS analysis of this cofactor-deficient VFe protein suggests that the P*-cluster differs from the standard [Fe_8S_7] structure of the P-cluster and likely consists of paired [Fe_4S_4]-like clusters [5].

observations point to a distinctive electronic structure of the V-cluster, which originates, at least in part, from the unique properties of V.

The striking homology between the primary sequences and the metal centers of V- and Mo-nitrogenases suggests that the V nitrogenase likely follows the same mode of action as its Mo counterpart during catalysis, forming a functional complex between its two component proteins to enable the ATP-dependent, inter-protein transfer of electrons from the [Fe_4S_4] center of the Fe protein, via the P*-cluster, to the V-cluster of the VFe protein for substrate reduction (Fig. 2). The overall homology in structure and mode-of-action renders a functional similarity between the V- and Mo-nitrogenases, which is reflected by the abilities of the two nitrogenases to catalyze the reduction of a similar set of substrates, such as N_2, H^+, C_2H_2 and CN^- [5]. However, the unique structural features of the V nitrogenase, including those of its P*- and V-clusters, as well as those of the protein environments surrounding these clusters, underlie the distinct catalytic properties of this nitrogenase. For example, it has been documented that the VFe protein is less efficient than the MoFe protein in reducing N_2, H^+ and C_2H_2 and, in the case of N_2 reduction, the VFe protein generates NH_3 and H_2 at a lower NH_3/H_2 ratio than its Mo counterpart.

But, perhaps the biggest difference between the catalytic properties of the V- and Mo-nitrogenases is their differential abilities to reduce CO and CO_2. The V nitrogenase is capable of reducing CO to hydrocarbons of up to C4 in length [*i.e.*, CH_4, C_2H_4, ethane (C_2H_6), propylene (C_3H_6), propane (C_3H_8), butylene (C_4H_8) and butane (C_4H_{10})] [29–31]. In comparison, except for CH_4, the Mo nitrogenase can generate the same set of hydrocarbons from CO reduction; however, the total amount of hydrocarbons formed by the Mo nitrogenase is only 0.1% of that by the V nitrogenase, and the product distribution and deuterium effect of the Mo nitrogenase-catalyzed reaction also clearly differ from those of the V nitrogenase-catalyzed reaction. Similarly, the V nitrogenase is able to reduce CO_2 to C1 (*i.e.*, CH_4) and C2 (*i.e.*, C_2H_4 and C_2H_6) hydrocarbons in the presence of D_2O, but it does not form hydrocarbons from CO_2 in the presence of H_2O. In contrast, the Mo nitrogenase is only capable of generating CH_4 in the presence of H_2O, yet the CH_4 generated in this case does not originate from CO_2 [27]. It should be noted that certain Mo nitrogenase variants have been shown to exhibit altered CO- and CO_2-reducing activities, although how substitution of one or two amino acid residues in the Mo nitrogenase could cause these changes remains unknown at the present time. What is known, however, is that synthetic V compounds are more active than synthetic Mo compounds in the reductive coupling of two CO moieties into functionalized acetylene ligands [56], which suggests that V (a group VB transition metal) is superior to Mo (a group VIB transition metal) in this particular type of reaction. Importantly, the ability of nitrogenase to form hydrocarbons from CO is analogous to the capacities of late transition metal catalysts in the industrial Fischer–Tropsch (FT) process [57]. However, contrary to the industrial process, the enzymatic reaction utilizes H^+ instead of H_2 (an expensive syngas) as the hydrogen source, and it occurs at room temperature and pressure, making it an appealing template for future development of energy-efficient approaches for CO-based hydrocarbon production [31].

The Iron (Fe)-only Nitrogenase

The Fe-only nitrogenase is the least understood of the three homologous nitrogenases. This enzyme has been isolated from *A. vinelandii*, *Rhodospirillum rubrum* and *Rhodobacter capsulatus* [2, 9, 10] and, like its Mo- and V-counterparts, it is a two-component system comprising the Fe protein and the iron-iron (FeFe) protein. The Fe protein of the Fe-only nitrogenase is encoded by *anfH* (also designated AnfH). An α_2-homodimer bridged by a [Fe_4S_4] cluster between the subunits, the *anfH*-encoded Fe protein shows a high degree of homology to both *nifH*- and *vnfH*-encoded Fe proteins, although the homology between the *anfH*-encoded Fe protein and *nifH*/*vnfH*-encoded Fe proteins is lower than that between the *nifH*- and *vnfH*-encoded Fe proteins. The FeFe protein of the Fe-only nitrogenase is the equivalent to the MoFe or VFe protein of the Mo- or V-nitrogenase. Like the VFe protein, the FeFe protein consists of α-, β- and δ-subunits, which are encoded by *anfD*, *anfK* and *anfG*, respectively. While progress has been made in improving the preparations of the FeFe protein from *R. capsulatus*, the successful purification of an intact form of this protein has remained a challenge and the most competent form of this protein reported so far has an $\alpha_2\beta_2\delta_2$-hexameric subunit composition [2]. EPR, Mössbauer and EXAFS studies of the *R. capsulatus* FeFe protein have provided spectroscopic evidence that this protein contains metal centers homologous to the P/P*-cluster (designated the P′-cluster) and the M/V-cluster (designated the FeFe cofactor or the Fe-cluster), respectively [58, 59]. Given the overall homology between the Fe-only nitrogenase and its Mo and V counterpart, this nitrogenase likely utilizes the same mode of action during catalysis, which involves complex formation between the two component proteins and electron transfer from the [Fe_4S_4] cluster of the Fe protein, via the P′-cluster, to the Fe-cluster of the FeFe protein, where substrate reduction takes place. Interestingly, the Fe-cluster may very well resemble a so-called L-cluster in composition and structure, with the latter being an Fe/S precursor that can be matured into an M-cluster on NifEN (see below).

The Nitrogenase Assembly Protein NifEN

NifEN is an indispensable assembly apparatus along the biosynthetic pathway of the M-cluster, receiving an Fe/S precursor from NifB and processing it further into an M-cluster before passing it on to the MoFe protein. Encoded by *nifE* and *nifN*, NifEN is an $\alpha_2\beta_2$-heterotetramer that shares a good degree of sequence homology with the MoFe protein [60, 61]. Sequence analysis reveals that NifEN contains cluster-binding sites that are homologous to those found in the MoFe protein: a “P-cluster” site at the interface of each $\alpha\beta$-subunit dimer, which houses a P-cluster analog; and an “M-cluster” site within each α-subunit, which houses the conversion of an Fe/S precursor to a mature M-cluster. Consistent with this observation, the “P-cluster” and the “M-cluster” in NifEN were identified by EPR, XAS/EXAFS and XES methods as a [Fe_4S_4]-type cluster [62] and an [Fe_8S_9C] cluster (designated the L-cluster) [63–65], respectively (Fig. 3A and B). Moreover, x-ray crystallographic analysis of an L-cluster-bound form of NifEN has further confirmed that the L-cluster is nearly indistinguishable in structure from the Fe/S core structure of the M-cluster [66, 67]; whereas biochemical experiments [68] have demonstrated that the NifEN-bound L-cluster can be converted to a fully matured M-cluster upon Fe protein-mediated

insertion of Mo and homocitrate prior to its delivery to its target binding site in the MoFe protein (Fig. 3C).

With a [Fe_4S_4] analog at the "P-cluster" site and an [Fe_8S_9C] homolog at the "M-cluster" site, NifEN has the equivalents (if simplified) for both clusters that are involved in the electron transfer within the MoFe protein (see Fig. 1). When combined with the Fe protein, NifEN is capable of reducing some of the substrates of Mo nitrogenase, such as C_2H_2 and N_3^-, albeit at much lower efficiencies than the Fe protein/MoFe protein system [69]. Like the Mo nitrogenase, the Fe protein/NifEN system requires the Fe protein to function as an ATP-dependent reductase and deliver electrons to NifEN for substrate reduction, as neither C_2H_2 nor N_3^- could be reduced by this enzymatic system if ATP was absent, if ATP was replaced by ADP or non hydrolyzable ATP analogs, or if the Fe protein was replaced by an Fe protein variant specifically defective in ATP hydrolysis [69]. Thus, formation of an Fe protein/NifEN complex that is homologous to the Fe protein/MoFe protein complex can be predicted during catalysis, which allows electrons to be transferred from the [Fe_4S_4] cluster of the Fe protein to the L-cluster of NifEN for substrate reduction (Fig. 3C).

There are, however, three interesting features of the Fe protein/NifEN system that set it apart from the Fe protein/MoFe protein system. One, the "P-cluster" analog in NifEN is a [Fe_4S_4]-type cluster, which is much simpler and, perhaps, far less efficient than the P-cluster ([Fe_8S_7]) in mediating the inter-protein electron transfer in this system. Two, the "M-cluster" homolog in NifEN is a Mo/homocitrate-free L-cluster ([Fe_8S_9C]), which is less complex and, possibly, less efficient than the M-cluster ([$MoFe_7S_9C$-homocitrate]) in catalyzing substrate reduction. Three, despite a similar location of the L- and M-clusters in their respective protein hosts, the L-cluster is nearly exposed at the surface of NifEN, whereas the M-cluster is buried within the MoFe protein. Taken together, these features contribute to the limited activity of the Fe protein/NifEN system in substrate reduction. However, such a "skeleton" system could be used to step-by-step add the "missing features" and address the functions of these features. Moreover, advantages could be taken of the slow turnover rates of the substrates by this enzymatic system, which may allow capture of substrates/intermediates for the subsequent mechanistic investigation.

The Protochlorophyllide Oxidoreductase (DPOR) and Chlorophyllide Oxidoreductase (COR)

The biosynthesis of chlorophylls and bacteriochlorophylls [70, 71] involves reduction of the C17–C18 double bond of protochlorophyllide (Pchlide) by dark operative protochlorophyllide oxidoreductase (DPOR) (Fig. 4A and B), which converts Pchlide to chlorophyllide (Chlide) (Fig. 4C). In addition, the biosynthesis of bactriochlorophylls specifically requires another reduction of the C7–C8 double bond by chlorophyllide oxidoreductase (COR), which converts Chlide into bacteriochlorophyllide (Bchlide) (Fig. 4C). The enzymes involved in these reductive steps along the biosynthetic pathway of chlorophylls and bacteriochlorophylls (encoded by *chl* and *bch*, respectively) share certain homology with nitrogenase enzymes (encoded by *nif*, *vnf* and *anf*, respectively). Like nitrogenases, DPOR or COR consists of two separately-purifiable, metallosulfur proteins: a homodimeric reductase component (encoded by *bchL*/*chlL* or *bchX*/*chlX*, respectively) that

shares up to 30% sequence identity with the Fe protein (encoded by *nifH*); and a heterotetrameric catalytic component (encoded by *bchNB*/*chlNB* or *bchYZ*/*chlYZ*, respectively) that shares up to 15% sequence identity with the MoFe protein (encoded by *nifDK*) [70]. Moreover, as is with the nitrogenase system, the two components of DPOR or COR form a functional complex during catalysis, which allows electron transfer from the reductase component to the catalytic component for the subsequent reduction of C17–C18 or C7–C8 double bond of the conjugated tetrapyrrole ring system [70].

Structural information has become available of the dimeric reductase component (designated the L_2 protein) and the heterotetrameric catalytic component (designated the N_2B_2 protein) of DPOR from various organisms in the recent years [72–75]. Together with the emerging biochemical data [76–81], these structural data have led to the elucidation of the mechanistic details of Chlide formation by DPOR. Like the Fe protein of nitrogenase, the L_2 protein belongs to a family of nucleotide-utilizing proteins, and it serves as an ATP-dependent reductase in Pchlide reduction. Encoded by *bchL/chlL*, the L_2 protein is a homodimer of *Mr* ~ 60 kDa. Each of its subunits has a binding site for MgATP, and the two subunits are bridged by a $[Fe_4S_4]$ cluster in between [72, 75]. The N_2B_2 protein is the catalytic partner of the L_2 protein in Pchlide reduction. It is an $\alpha_2\beta_2$-tetramer of *Mr* ~ 210 kDa, and its α-and β-subunits are encoded by *bchN/chlN* and *bchB/chlB*, respectively [76–81]. The N_2B_2 protein contains, in each $\alpha\beta$-subunit pair, one $[Fe_4S_4]$ cluster that is bridged between the α- and β-subunits, and one binding site for Pchlide that is mainly located within the α-subunit but also capped by the β-subunit [72–74]. Binding of Pchlide to the N_2B_2 protein is required for the formation of DPOR complex [79], and hydrolysis of ATP is believed to facilitate the association and dissociation between the L_2 protein and the N_2B_2 protein [72, 79]. Consistent with this hypothesis, the x-ray crystal structure of a MgADP·AlF_4^--stabilized complex between the L_2 protein and the N_2B_2 protein from *Prochlorococcus marinus* [72] suggests that electrons are transferred sequentially from the $[Fe_4S_4]$ cluster of the L_2 protein, via the $[Fe_4S_4]$ cluster of the N_2B_2 protein, to Pchlide (Fig. 4A and B), which allows the reduction to occur at the C17–C18 position of its tetrapyrrole ring (Fig. 4C).

The reaction catalyzed by DPOR is depicted as follows: Pchlide + $2H^+$ + 4MgATP + $2e^-$ → Chlide + 4MgADP + $4P_i$ [72]. Interestingly, DPOR is capable of catalyzing the two-electron reduction of N_3^- or N_2H_4 to NH_3, which mirrors the ability of nitrogenase to catalyze the reduction of the same substrates [72]. However, despite sharing the two “simple” substrates with nitrogenase, DPOR is unable to reduce the more “complex” substrates of nitrogenase, such as N_2 [1] and CO [29, 31], which require the transfer of more than two electrons through the enzymatic system. The narrow substrate spectrum of these two systems likely originates from the presence of a $[Fe_4S_4]$ clusters instead of a high-nuclearity, $[Fe_8S_7]$ cluster at its “P-cluster” site. Nevertheless, the striking similarities between the structures and functions of DPOR and nitrogenases point to a strong evolutionary tie between the two enzyme systems.

Compared to the well-studied DPOR system, information of the dimeric, reductase component (designated the X_2 protein) and the heterotetrameric, catalytic component (designated the Y_2Z_2 protein) of the COR system has remained scarce. However, the homology between COR and DPOR suggests a close resemblance between the reactions

catalyzed by these two enzyme systems [70, 82]. The *bchYZ*- and *bchX*-encoded subunits of COR share sequence identity of up to 22% and 35%, respectively, with the *bchNB*- and *bchL*-encoded subunits of DPOR [70]. Sequence alignments between the *bchX*- and *chlL*/*bchL*-encoded subunits indicate that both the Cys ligands of the [Fe_4S_4] cluster and the ATP-binding sites are conserved in these proteins [83]. Moreover, as observed in the case of the L_2 protein, EPR analysis revealed signals consistent with the presence of a [Fe_4S_4] cluster in the X_2 protein [70]; whereas biochemical experiments demonstrated that the L_2 protein could be replaced by X_2 protein in the activity assay of DPOR when Pchlide was supplied as a substrate [78]. Similarly, sequence analysis of the Y_2Z_2 protein suggests the presence of Cys ligands for [Fe_4S_4] clusters at locations comparable to those in the N_2B_2 protein. Consistent with this observation, EPR experiments further revealed the presence of a redox-active [Fe_4S_4] cluster in the Y_2Z_2 protein [78]. Together, these results strongly suggest that COR employs a highly similar mechanism to DPOR for the reduction of the tetrapyrrole substrate.

The Nitrogen-Fixation-Like (Nfl) Proteins

Genomic analysis indicates the presence of *nifH*-like and *nifD*/*nifK*-like genes among all methanogenic microbes [84]. These genes clearly differ from the other sets of genes that encode proteins for nitrogen fixation in methanogenic organisms. Phylogenetic analysis has led to the conclusion that the *nif*-like sequences *n* H and *n* D (*n* stands for ***n***itrogen ***f***ixation ***l***ike) lie basal in the tree between the nitrogenase and the DPOR/COR clades [84], and another study has suggested that the two *nfl*-encoded proteins form an enzymatic system that represents a “simplified”, ancestral member of this family of homologous enzymes [85]. Sequence alignments between the *nflH*-encoded protein (also designated NflH), the Fe protein and the L_2 protein reveal the presence of a conserved ATP-binding site in the three proteins; moreover, they reveal the presence of two conserved cysteine residues from each subunit that could coordinate an analogous [Fe_4S_4] cluster at the interfaces of these dimeric proteins (Fig. 5A). The *n D*-encoded protein (designated NflD), on the other hand, is somewhat different from the *nifD*- and *chlN*/*bchN*-encoded proteins based on sequence analysis, as none of the ligands for the M-cluster can be found in the sequence of the *nflD*-encoded protein. Interestingly, some cysteine residues that ligate the P-cluster in the MoFe protein are conserved in the *nflD*-encoded sequence, which would be sufficient for the ligation of a [Fe_4S_4] cluster between the two subunits of a dimeric form of the *nflD*-encode protein (Fig. 5A).

Initial information regarding the functions of the *nfl*-encoded proteins has been obtained through studies of *Methanocaldococcus jannaschii*, a methanogenic microbe that does not perform nitrogen xation or photosynthesis [70]. These studies have shown that the *n H*- and *n D*-encoded proteins interact with each other and that both proteins are expressed constitutively and independently of the availability of nitrogen. Combined with what is known about the homologous DPOR/COR systems, these observations have led to the speculation that the enzyme system comprising *nflH*- and *nflD*-encoded proteins may be involved in the biosynthesis of cofactor F430, the active site of methyl-coenzyme M reductase that catalyzes the final step of methanogenesis. Given the homology between the *nfl*- and *bch*/*chl* systems, it appears possible that the *nflD*- and *nflH*-encoded proteins could

work together and catalyze one or more ring reduction steps that are required for the biosynthesis of cofactor F430 [86] and that the catalytic mechanism of this system likely mirrors that of the DPOR or COR system, which involves inter-protein electron transfer from the reductase component (the *niflH*-encoded protein) to the catalytic component (the *nflD*-encoded protein) and the subsequent substrate reduction at its binding site in the *nflD*-encoded protein (Fig. 5B). Clearly, further investigation is required to test this hypothesis and elucidate the functions of the *nfl*-encoded proteins. Perhaps more importantly, these studies may help establish an interesting evolutionary link between proteins involved in methanogenesis (Nfl), bacterial photosynthesis (Bch/Chl) and nitrogen fixation (Nif), which are the three key metabolic processes central to the emergence of life on Earth.

Acknowledgments

This work was supported by National Institutes of Health grant GM 67626 (M.W.R.).

Abbreviations

Fe protein	iron protein
MoFe protein	molybdenum-iron protein
VFe protein	vanadium-iron protein
FeFe protein	iron-iron protein
EPR	electron paramagnetic resonance
XAS	x-ray absorption spectroscopy
SAXS	small angle x-ray scattering
EXAFS	extended x-ray absorption fine structure
XES	x-ray emission spectroscopy
ENDOR	electron-nuclear double resonance
ESEEM	electron spin echo envelope modulation

References

1. Burgess BK, Lowe DJ. Mechanism of molybdenum nitrogenase. Chem Rev. 1996; 96:2983–3012. [PubMed: 11848849]
2. Eady RR. Structure-function relationships of alternative nitrogenases. Chem Rev. 1996; 96:3013–3030. [PubMed: 11848850]
3. Rees DC, Akif Tezcan F, Haynes CA, Walton MY, Andrade S, Einsle O, Howard JB. Structural basis of biological nitrogen fixation. Philos Trans A Math Phys Eng Sci. 2005; 363:971–984. [PubMed: 15901546]
4. Hoffman BM, Lukoyanov D, Yang ZY, Dean DR, Seefeldt LC. Mechanism of nitrogen fixation by nitrogenase: the next stage. Chem Rev. 2014; 114:4041–4062. [PubMed: 24467365]
5. Hu Y, Lee CC, Ribbe MW. Vanadium nitrogenase: a two-hit wonder? Dalton Trans. 2012; 41:1118–1127. [PubMed: 22101422]
6. Reinbothe C, El Bakkouri M, Buhr F, Muraki N, Nomata J, Kurisu G, Fujita Y, Reinbothe S. Chlorophyll biosynthesis: spotlight on protochlorophyllide reduction. Trends Plant Sci. 2010; 15:614–624. [PubMed: 20801074]

7. Moser J, Bröcker MJ. Enzymatic systems with homology to nitrogenase. Methods Mol Biol. 2011; 766:67–77. [PubMed: 21833861]
8. Christiansen J, Dean DR, Seefeldt LC. Mechanistic features of the Mo-containing nitrogenase. Annu Rev Plant Physiol Plant Mol Biol. 2001; 52:269–295. [PubMed: 11337399]
9. Lawson DM, Smith BE. Molybdenum nitrogenases: a crystallographic and mechanistic view. Met Ions Biol Syst. 2002; 39:75–119. [PubMed: 11913144]
10. Eady RR. Vanadium nitrogenases of Azotobacter. Met Ions Biol Syst. 1995; 31:363–405. [PubMed: 8564813]
11. Howard JB, Rees DC. Structural basis of biological nitrogen fixation. Chem Rev. 1996; 96:2965–2982. [PubMed: 11848848]
12. Georgiadis MM, Komiya H, Chakrabarti P, Woo D, Kornuc JJ, Rees DC. Crystallographic structure of the nitrogenase iron protein from *Azotobacter vinelandii*. Science. 1992; 257:1653–1659. [PubMed: 1529353]
13. Kim J, Rees DC. Structural models for the metal centers in the nitrogenase molybdenum-iron protein. Science. 1992; 257:1677–1682. [PubMed: 1529354]
14. Chan MK, Kim J, Rees DC. The nitrogenase FeMo-cofactor and P-cluster pair: 2.2 A resolution structures. Science. 1993; 260:792–794. [PubMed: 8484118]
15. Schindelin H, Kisker C, Schlessman JL, Howard JB, Rees DC. Structure of ADP x AlF_4^--stabilized nitrogenase complex and its implications for signal transduction. Nature. 1997; 387:370–376. [PubMed: 9163420]
16. Einsle O, Tezcan FA, Andrade SL, Schmid B, Yoshida M, Howard JB, Rees DC. Nitrogenase MoFe-protein at 1.16 A resolution: a central ligand in the FeMo-cofactor. Science. 2002; 297:1696–1700. [PubMed: 12215645]
17. Spatzal T, Aksoyoglu M, Zhang L, Andrade SL, Schleicher E, Weber S, Rees DC, Einsle O. Evidence for interstitial carbon in nitrogenase FeMo cofactor. Science. 2011; 334:940. [PubMed: 22096190]
18. Chen L, Gavini N, Tsuruta H, Eliezer D, Burgess BK, Doniach S, Hodgson KO. MgATP-induced conformational changes in the iron protein from *Azotobacter vinelandii*, as studied by small-angle x-ray scattering. J Biol Chem. 1994; 269:3290–3294. [PubMed: 8106367]
19. Eady RR. Current status of structure function relationships of vanadium nitrogenase. Coord Chem Rev. 2003; 237:23–30.
20. Lee HI, Hales BJ, Hoffman BM. Metal-ion valencies of the FeMo cofactor in CO-inhibited and resting state nitrogenase by Fe-57 Q-band ENDOR. J Am Chem Soc. 1997; 119:11395–11400.
21. Christie PD, Lee HI, Cameron LM, Hales BJ, Orme-Johnson WH, Hoffman BM. Identification of the CO-binding cluster in nitrogenase MoFe protein by ENDOR of Fe-57 isotopomers. J Am Chem Soc. 1996; 118:8707–8709.
22. Pollock RC, Lee HI, Cameron LM, Derose VI, Hales BJ, Orme-Johnson WH, Hoffman BM. Investigation of co bound to inhibited forms of nitrogenase MoFe protein by C-13 ENDOR. J Am Chem Soc. 1995; 117:8686–8687.
23. Lee HI, Cameron LM, Hales BJ, Hoffman BM. CO binding to the FeMo cofactor of CO-inhibited nitrogenase: (CO)-C-13 and H-1 Q-band ENDOR investigation. J Am Chem Soc. 1997; 119:10121–10126.
24. Lee HI, Sorlie M, Christiansen J, Song RT, Dean DR, Hales BJ, Hoffman BM. Characterization of an intermediate in the reduction of acetylene by the nitrogenase alpha-Gln(195) MoFe protein by Q-band EPR and C-13, H-1 ENDOR. J Am Chem Soc. 2000; 122:5582–5587.
25. Conradson SD, Burgess BK, Vaughn SA, Roe AL, Hedman B, Hodgson KO, Holm RH. Cyanide and methylisocyanide binding to the isolated iron-molybdenum cofactor of nitrogenase. J Biol Chem. 1989; 264:15967–15974. [PubMed: 2777773]
26. Ibrahim SK, Vincent K, Gormal CA, Smith BE, Best SP, Pickett CJ. The isolated iron-molybdenum cofactor of nitrogenase binds carbon monoxide upon electrochemically accessing reduced states. Chem Commun. 1999; 11:1019–1020.
27. Rebelein JG, Hu Y, Ribbe MW. Differential Reduction of CO_2 by Molybdenum and Vanadium Nitrogenases. Angew Chem Int Ed Engl. 201410.1002/anie.201406863

28. Lee CC, Hu Y, Ribbe MW. ATP-independent formation of hydrocarbons catalyzed by isolated nitrogenase cofactors. Angew Chem Int Ed Engl. 2012; 51:1947–1949. [PubMed: 22253035]
29. Hu Y, Lee CC, Ribbe MW. Extending the carbon chain: hydrocarbon formation catalyzed by vanadium/molybdenum nitrogenases. Science. 2011; 333:753–755. [PubMed: 21817053]
30. Lee CC, Hu Y, Ribbe MW. Tracing the hydrogen source of hydrocarbons formed by vanadium nitrogenase. Angew Chem Int Ed Engl. 2011; 50:5545–5547. [PubMed: 21538750]
31. Lee CC, Hu Y, Ribbe MW. Vanadium nitrogenase reduces CO. Science. 2010; 329:642. [PubMed: 20689010]
32. Yang ZY, Moure VR, Dean DR, Seefeldt LC. Carbon dioxide reduction to methane and coupling with acetylene to form propylene catalyzed by remodeled nitrogenase. Proc Natl Acad Sci U S A. 2012; 109:19644–19648. [PubMed: 23150564]
33. Yang ZY, Dean DR, Seefeldt LC. Molybdenum nitrogenase catalyzes the reduction and coupling of CO to form hydrocarbons. J Biol Chem. 2011; 286:19417–19421. [PubMed: 21454640]
34. Hoffman BM, Lukoyanov D, Yang ZY, Dean DR, Seefeldt LC. Mechanism of nitrogen fixation by nitrogenase: the next stage. Chem Rev. 2014; 114:4041–4062. [PubMed: 24467365]
35. Lancaster KM, Roemelt M, Ettenhuber P, Hu Y, Ribbe MW, Neese F, Bergmann U, DeBeer S. X-ray emission spectroscopy evidences a central carbon in the nitrogenase iron-molybdenum cofactor. Science. 2011; 334:974–977. [PubMed: 22096198]
36. Wiig JA, Hu Y, Lee CC, Ribbe MW. Radical SAM-dependent carbon insertion into the nitrogenase M-cluster. Science. 2012; 337:1672–1675. [PubMed: 23019652]
37. Wiig JA, Lee CC, Hu Y, Ribbe MW. Tracing the interstitial carbide of the nitrogenase cofactor during substrate turnover. J Am Chem Soc. 2013; 135:4982–4983. [PubMed: 23514429]
38. Moret ME, Peters JC. N_2 functionalization at iron metallaboratranes. J Am Chem Soc. 2011; 133:18118–18121. [PubMed: 22008018]
39. Bortels H. Kurze Notiz über die Katalyse der biologischen Stickstoffbindung. Zentralbl Bakt II Abt. 1933; 87:476–477.
40. Eady RR, Robson RL, Richardson TH, Miller RW, Hawkins M. The vanadium nitrogenase of *Azotobacter chroococcum*. Purification and properties of the VFe protein. Biochem J. 1987; 244:197–207. [PubMed: 2821997]
41. Eady RR, Richardson TH, Miller RW, Hawkins M, Lowe DJ. The vanadium nitrogenase of *Azotobacter chroococcum*. Purification and properties of the Fe protein. Biochem J. 1988; 256:189–196. [PubMed: 2851977]
42. Robson RL, Eady RR, Richardson TH, Miller RW, Hawkins M, Postgate JR. The alternative nitrogenase of *Azotobacter chroococcum* is a vanadium enzyme. Nature. 1986; 322:388–390.
43. Hales BJ, Case EE, Morningstar JE, Dzeda MF, Mauterer LA. Isolation of a new vanadium-containing nitrogenase from *Azotobacter vinelandii*. Biochemistry. 1986; 25:7251–7255. [PubMed: 3026449]
44. Hales BJ, Langosch DJ, Case EE. Isolation and characterization of a second nitrogenase Fe-protein from *Azotobacter vinelandii*. J Biol Chem. 1986; 261:15301–15306. [PubMed: 3021770]
45. Blanchard CZ, Hales BJ. Isolation of two forms of the nitrogenase VFe protein from *Azotobacter vinelandii*. Biochemistry. 1996; 35:472–478. [PubMed: 8555217]
46. Lee CC, Hu Y, Ribbe MW. Unique features of the nitrogenase VFe protein from *Azotobacter vinelandii*. Proc Natl Acad Sci U S A. 2009; 106:9209–9214. [PubMed: 19478062]
47. Blank MA, Lee CC, Hu Y, Hodgson KO, Hedman B, Ribbe MW. Structural models of the $[Fe_4S_4]$ clusters of homologous nitrogenase Fe proteins. Inorg Chem. 2011; 50:7123–7128. [PubMed: 21718019]
48. Morningstar JE, Johnson MK, Case EE, Hales BJ. Characterization of the metal clusters in the nitrogenase molybdenum-iron and vanadium-iron proteins of *Azotobacter vinelandii* using magnetic circular dichroism spectroscopy. Biochemistry. 1987; 26:1795–1800. [PubMed: 3474027]
49. Tittsworth RC, Hales BJ. Oxidative titration of the nitrogenase VFe protein from *Azotobacter vinelandii*: an example of redox-gated electron flow. Biochemistry. 1996; 35:479–487. [PubMed: 8555218]

50. Hu Y, Corbett MC, Fay AW, Webber JA, Hedman B, Hodgson KO, Ribbe MW. Nitrogenase reactivity with P-cluster variants. Proc Natl Acad Sci U S A. 2005; 27:13825–13830. [PubMed: 16166259]
51. Chen J, Christiansen J, Tittsworth RC, Hales BJ, George GN, Coucouvanis D, Cramer SP. Iron EXAFS of Azotobacter vinelandii nitrogenase MoFe and VFe proteins. J Am Chem Soc. 1993; 115:5509–5515.
52. Harvey I, Arber JM, Eady RR, Smith BE, Garner CD, Hasnain SS. Iron K-edge X-ray-absorption spectroscopy of the iron-vanadium cofactor of the vanadium nitrogenase from *Azotobacter chroococcum*. Biochem J. 1990; 266:929–931. [PubMed: 2327976]
53. Arber JM, Dobson BR, Eady RR, Stevens P, Hasnain SS, Garner CD, Smith BE. Vanadium k-edge x-ray absorption spectrum of the VFe protein of the vanadium nitrogenase of *Azotobacter chroococum*. Nature. 1987; 325:372–374.
54. George GN, Coyle CL, Hales BJ, Cramer SP. X-ray absorption of *Azotobacter vinelandii* vanadium nitrogenase. J Am Chem Soc. 1988; 110:4057–4059.
55. Fay AW, Blank MA, Lee CC, Hu Y, Hodgson KO, Hedman B, Ribbe MW. Characterization of isolated nitrogenase FeVco. J Am Chem Soc. 2010; 132:12612–12618. [PubMed: 20718463]
56. Carnahan EC, Protasiewicz JD, Lippard SJ. 15 years of reductive coupling - what have we learned. Acc Chem Res. 1993; 26:90–97.
57. Rofer-DePoorter CK. A comprehensive mechanism for the Fischer-Tropsch synthesis. Chem Rev. 1981; 81:447–474.
58. Siemann S, Schneider K, Dröttboom M, Müller A. The Fe-only nitrogenase and the Mo nitrogenase from *Rhodobacter capsulatus*: a comparative study on the redox properties of the metal clusters present in the dinitrogenase components. Eur J Biochem. 2002; 269:1650–1661. [PubMed: 11895435]
59. Krahn E, Weiss R, Kröckel M, Groppe J, Henkel G, Cramer P, Trautwein X, Schneider K, Müller A. The Fe-only nitrogenase from *Rhodobacter capsulatus*: identification of the cofactor, an unusual, high-nuclearity iron-sulfur cluster, by Fe K-edge EXAFS and 57Fe Mössbauer spectroscopy. J Biol Inorg Chem. 2002; 7:37–45. [PubMed: 11862539]
60. Dos Santos PC, Dean DR, Hu Y, Ribbe MW. Formation and insertion of the nitrogenase iron-molybdenum cofactor. Chem Rev. 2004; 104:1159–1173. [PubMed: 14871152]
61. Hu Y, Fay AW, Lee CC, Yoshizawa J, Ribbe MW. Assembly of nitrogenase MoFe protein. Biochemistry. 2008; 47:3973–3981. [PubMed: 18314963]
62. Goodwin PJ, Agar JN, Roll JT, Roberts GP, Johnson MK, Dean DR. The *Azotobacter vinelandii* NifEN complex contains two identical [4Fe-4S] clusters. Biochemistry. 1998; 37:10420–10428. [PubMed: 9671511]
63. Hu Y, Fay AW, Ribbe MW. Identification of a nitrogenase FeMo cofactor precursor on NifEN complex. Proc Natl Acad Sci U S A. 2005; 102:3236–3241. [PubMed: 15728375]
64. Corbett MC, Hu Y, Fay AW, Ribbe MW, Hedman B, Hodgson KO. Structural insights into a protein-bound iron-molybdenum cofactor precursor. Proc Natl Acad Sci U S A. 2006; 103:1238–1243. [PubMed: 16423898]
65. Lancaster KM, Hu Y, Bergmann U, Ribbe MW, DeBeer S. X-ray spectroscopic observation of an interstitial carbide in NifEN-bound FeMoco precursor. J Am Chem Soc. 2013; 135:610–612. [PubMed: 23276198]
66. Fay AW, Blank MA, Lee CC, Hu Y, Hodgson KO, Hedman B, Ribbe MW. Spectroscopic characterization of the isolated iron-molybdenum cofactor (FeMoco) precursor from the protein NifEN. Angew Chem Int Ed Engl. 2011; 50:7787–7790. [PubMed: 21726031]
67. Kaiser JT, Hu Y, Wiig JA, Rees DC, Ribbe MW. Structure of precursor-bound NifEN: a nitrogenase FeMo cofactor maturase/insertase. Science. 2011; 331:91–94. [PubMed: 21212358]
68. Hu Y, Corbett MC, Fay AW, Webber JA, Hodgson KO, Hedman B, Ribbe MW. FeMo cofactor maturation on NifEN. Proc Natl Acad Sci U S A. 2006; 103:17119–17124. [PubMed: 17050696]
69. Hu Y, Yoshizawa JM, Fay AW, Lee CC, Wiig JA, Ribbe MW. Catalytic activities of NifEN: implications for nitrogenase evolution and mechanism. Proc Natl Acad Sci U S A. 2009; 106:16962–16966. [PubMed: 19805110]

70. Moser J, Bröcker MJ. Enzymatic systems with homology to nitrogenase. Methods Mol Biol. 2011; 766:67–77. [PubMed: 21833861]
71. Reinbothe C, El Bakkouri M, Buhr F, Muraki N, Nomata J, Kurisu G, Fujita Y, Reinbothe S. Chlorophyll biosynthesis: spotlight on protochlorophyllide reduction. Trends Plant Sci. 2010; 15:614–624. [PubMed: 20801074]
72. Moser J, Lange C, Krausze J, Rebelein J, Schubert WD, Ribbe MW, Heinz DW, Jahn D. Structure of ADP-aluminium fluoride-stabilized protochlorophyllide oxidoreductase complex. Proc Natl Acad Sci U S A. 2013; 110:2094–2098. [PubMed: 23341615]
73. Bröcker MJ, Schomburg S, Heinz DW, Jahn D, Schubert WD, Moser J. Crystal structure of the nitrogenase-like dark operative protochlorophyllide oxidoreductase catalytic complex (ChlN/ChlB)$_2$. J Biol Chem. 2010; 285:27336–27345. [PubMed: 20558746]
74. Muraki N, Nomata J, Ebata K, Mizoguchi T, Shiba T, Tamiaki H, Kurisu G, Fujita Y. X-ray crystal structure of the light-independent protochlorophyllide reductase. Nature. 2010; 465:110–114. [PubMed: 20400946]
75. Sarma R, Barney BM, Hamilton TL, Jones A, Seefeldt LC, Peters JW. Crystal structure of the L protein of Rhodobacter sphaeroides light-independent protochlorophyllide reductase with MgADP bound: a homologue of the nitrogenase Fe protein. Biochemistry. 2008; 47:13004–13015. [PubMed: 19006326]
76. Bröcker MJ, Virus S, Ganskow S, Heathcote P, Heinz DW, Schubert WD, Jahn D, Moser J. ATP-driven reduction by dark-operative protochlorophyllide oxidoreductase from Chlorobium tepidum mechanistically resembles nitrogenase catalysis. J Biol Chem. 2008; 283:10559–10567. [PubMed: 18252716]
77. Bröcker MJ, Wätzlich D, Uliczka F, Virus S, Saggu M, Lendzian F, Scheer H, Rüdiger W, Moser J, Jahn D. Substrate recognition of nitrogenase-like dark operative protochlorophyllide oxidoreductase from Prochlorococcus marinus. J Biol Chem. 2008; 283:29873–29881. [PubMed: 18693243]
78. Wätzlich D, Bröcker MJ, Uliczka F, Ribbe M, Virus S, Jahn D, Moser J. Chimeric nitrogenase-like enzymes of (bacterio)chlorophyll biosynthesis. J Biol Chem. 2009; 284:15530–15540. [PubMed: 19336405]
79. Bröcker MJ, Wätzlich D, Saggu M, Lendzian F, Moser J, Jahn D. Biosynthesis of (bacterio)chlorophylls: ATP-dependent transient subunit interaction and electron transfer of dark operative protochlorophyllide oxidoreductase. J Biol Chem. 2010; 285:8268–8277. [PubMed: 20075073]
80. Fujita Y, Bauer CE. Reconstitution of light-independent protochlorophyllide reductase from purified bchl and BchN-BchB subunits. In vitro confirmation of nitrogenase-like features of a bacteriochlorophyll biosynthesis enzyme. J Biol Chem. 2000; 275:23583–23588. [PubMed: 10811655]
81. Nomata J, Kitashima M, Inoue K, Fujita Y. Nitrogenase Fe protein-like Fe-S cluster is conserved in L-protein (BchL) of dark-operative protochlorophyllide reductase from *Rhodobacter capsulatus*. FEBS Lett. 2006; 580:6151–6154. [PubMed: 17064695]
82. Nomata J, Mizoguchi T, Tamiaki H, Fujita Y. A second nitrogenase-like enzyme for bacteriochlorophyll biosynthesis: reconstitution of chlorophyllide a reductase with purified X-protein (BchX) and YZ-protein (BchY-BchZ) from *Rhodobacter capsulatus*. J Biol Chem. 2006; 281:15021–15028. [PubMed: 16571720]
83. Burke DH, Hearst JE, Sidow A. Early evolution of photosynthesis: clues from nitrogenase and chlorophyll iron proteins. Proc Natl Acad Sci U S A. 1993; 90:7134–7138. [PubMed: 8346226]
84. Raymond J, Siefert JL, Staples CR, Blankenship RE. The natural history of nitrogen fixation. Mol Biol Evol. 2004; 21:541–554. [PubMed: 14694078]
85. Boyd ES, Peters JW. New insights into the evolutionary history of biological nitrogen fixation. Front Microbiol. 2013; 4:201. [PubMed: 23935594]
86. Staples CR, Lahiri S, Raymond J, Von Herbulis L, Mukhophadhyay B, Blankenship RE. Expression and association of group IV nitrogenase NifD and NifH homologs in the non-nitrogen-fixing archaeon *Methanocaldococcus jannaschii*. J Bacteriol. 2007; 189:7392–7398. [PubMed: 17660283]

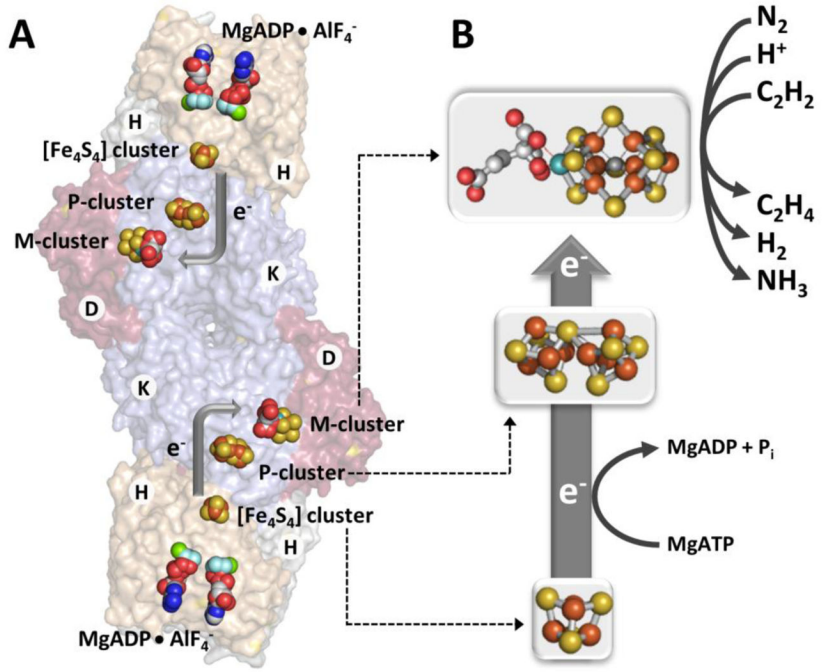

Fig. 1.

(A) Surface presentation (transparent) of the structure of the MgADP•AlF_4^--stabilized Fe protein/MoFe protein complex. MgADP•AlF_4^-, [Fe_4S_4] cluster, P-cluster and M-cluster are shown as space-filling models. The two subunits of the Fe protein (labeled as H) are colored gray and light wheat, respectively, and the α- and β-subunits of the MoFe protein are colored red (labeled as D) and light blue (labeled as K), respectively. **(B)** Components involved in electron transfer during catalysis. All clusters are shown as ball-and-stick models. Atoms are colored as follows: Fe, orange; S, yellow; Mo, cyan; O, red; C, gray; N, blue; Mg, dark green; Al, light green; F, light blue. PYMOL was used to create this figure (PDB IDs: 1N2C, 3U7Q).

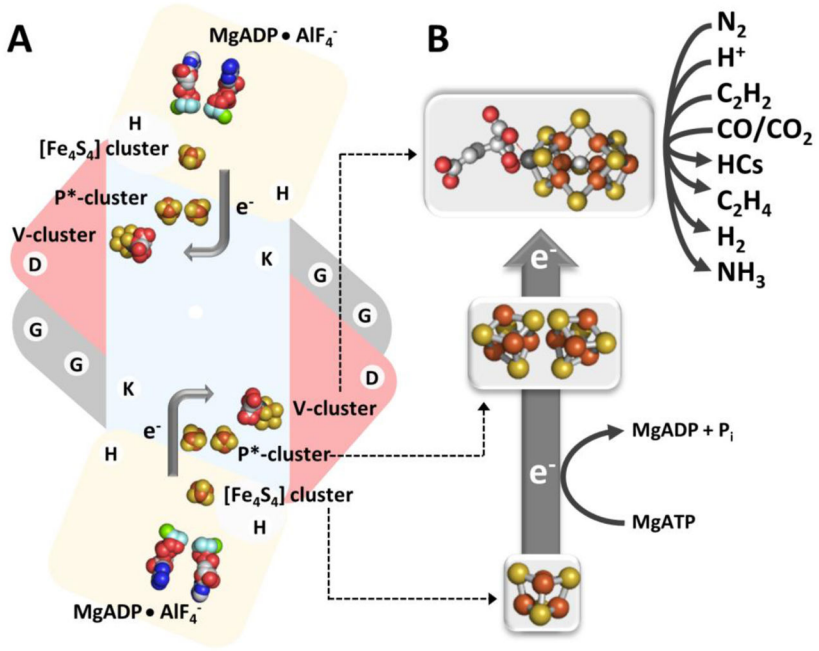

Fig. 2.

(A) Schematic presentation (transparent) of the hypothetical structural layout of the MgADP•AlF_4^--stabilized Fe protein/VFe protein complex. MgADP•AlF_4^-, $[Fe_4S_4]$ cluster, P*-cluster and V-cluster are shown as space-filling models. The two subunits of the Fe protein (labeled as H) are colored gray and light wheat, respectively, and the α-, β- and δ-subunits of the MoFe protein are colored red (labeled as D), light blue (labeled as K) and dark gray (labeled as G), respectively. **(B)** Components involved in electron transfer during catalysis. All clusters are shown as ball-and-stick models. The structures of the clusters are derived from the available XAS/EXAFS and XES data. Atoms are colored as follows: Fe, orange; S, yellow; V, dark gray; O, red; C, gray; N, blue; Mg, dark green; Al, light green; F, light blue. HCs, hydrocarbons.

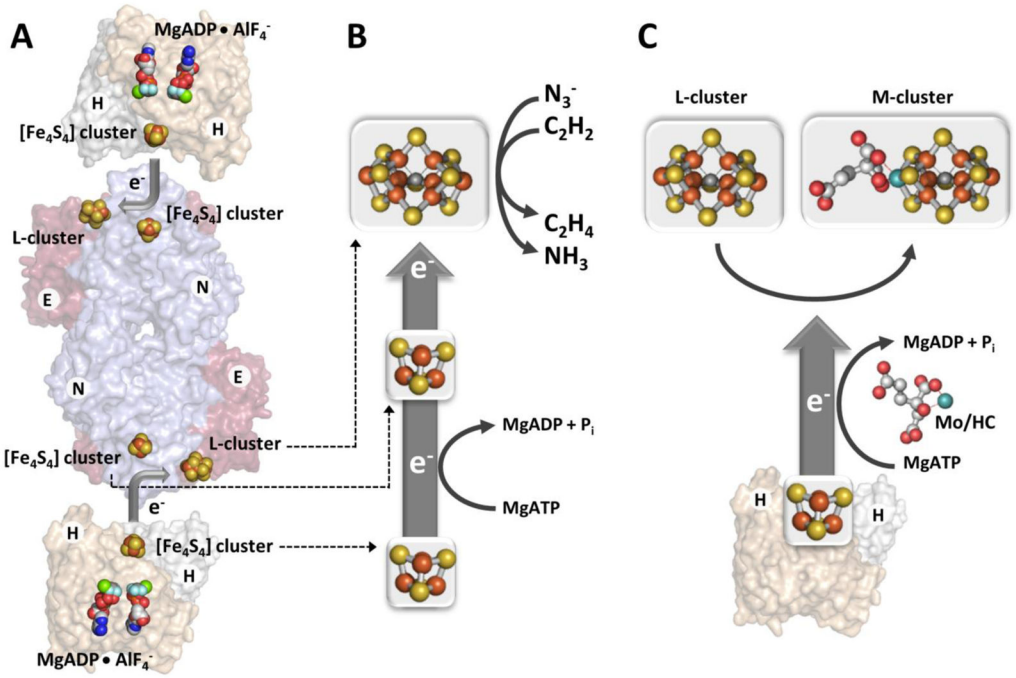

Fig. 3.

(A) Surface presentation (transparent) of the hypothetical structural layout of the MgADP•AlF_4^--stabilized Fe protein/NifEN complex. MgADP•AlF_4^-, [Fe_4S_4] clusters and L-cluster are shown as space-filling models. The two subunits of the Fe protein (labeled as H) are colored gray and light wheat, respectively, and the α- and β-subunits of the NifEN are colored red (labeled as E) and light blue (labeled as N), respectively. **(B)** Components involved in electron transfer during catalysis. All clusters are shown as ball-and-stick models. **(C)** Schematic presentation of the conversion of L- to M-cluster (C, top) on NifEN upon the replacement of a terminal Fe atom by Mo and homocitrate (HC). The Fe protein (C, bottom) serves as an ATP-dependent Mo/HC insertase in this process. Atoms are colored as follows: Fe, orange; S, yellow; O, red; C, gray; N, blue; Mg, dark green; Al, light green; F, light blue. PYMOL was used to create this figure (PDB IDs: 1N2C, 3PDI).

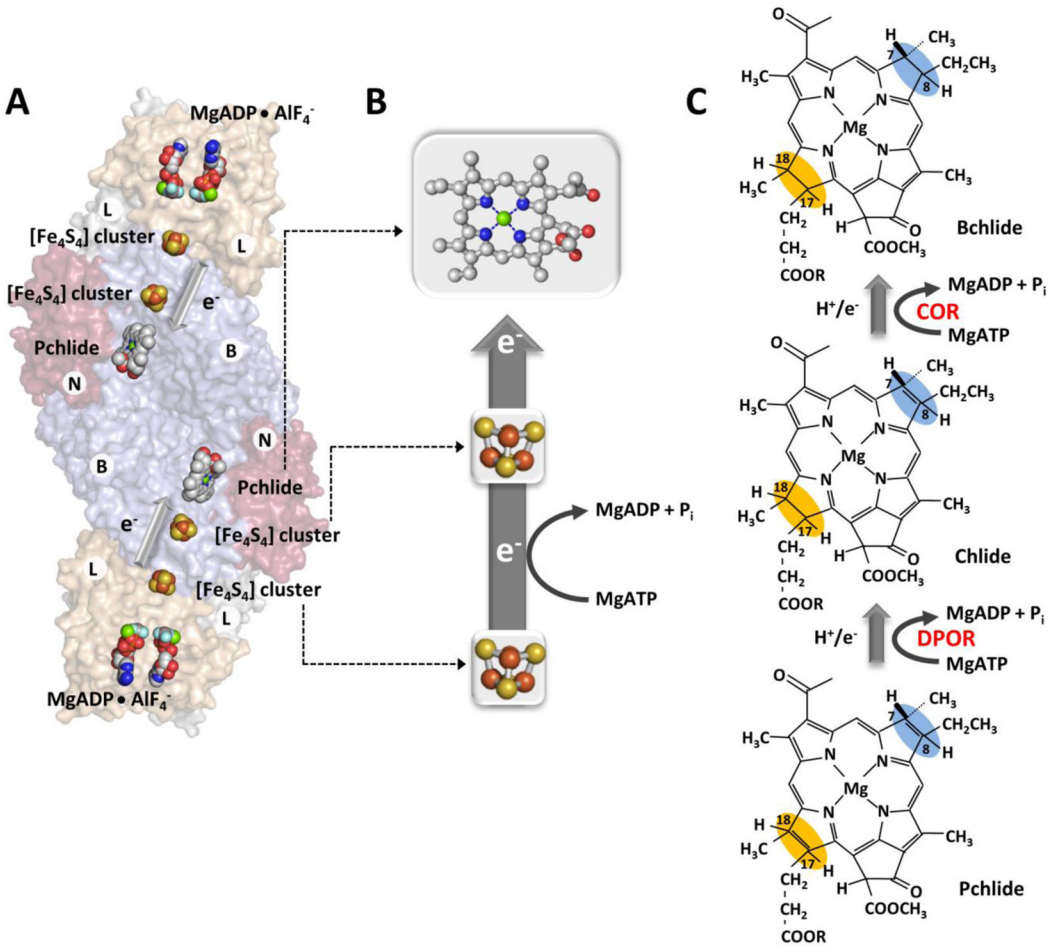

Fig. 4.

(A) Surface presentation (transparent) of the structure of the MgADP•AlF_4^--stabilized ChlL/ChlNB complex. MgADP•AlF_4^-, $[Fe_4S_4]$ clusters and Pchlide are shown as space-filling models. The two subunits of ChlL (labeled as L) are colored gray and light wheat, respectively, and the α- and β-subunits of ChlNB are colored red (labeled as N) and light blue (labeled as B), respectively. **(B)** Components involved in electron transfer during catalysis. All clusters and Pchlide are shown as ball-and-stick models. Atoms are colored as follows: Fe, orange; S, yellow; O, red; C, gray; N, blue; Mg, dark green; Al, light green; F, light blue. PYMOL was used to create this figure (PDB ID: 2YNM). **(C)** DPOR catalyzes the formation of Chlide through ATP-dependent, stereospecific reduction of the C17–C18 double bond of Pchlide, while COR catalyzes the formation of Bchlide through ATP-dependent, stereospecific reduction of the C7–C8 double bond of Chlide,

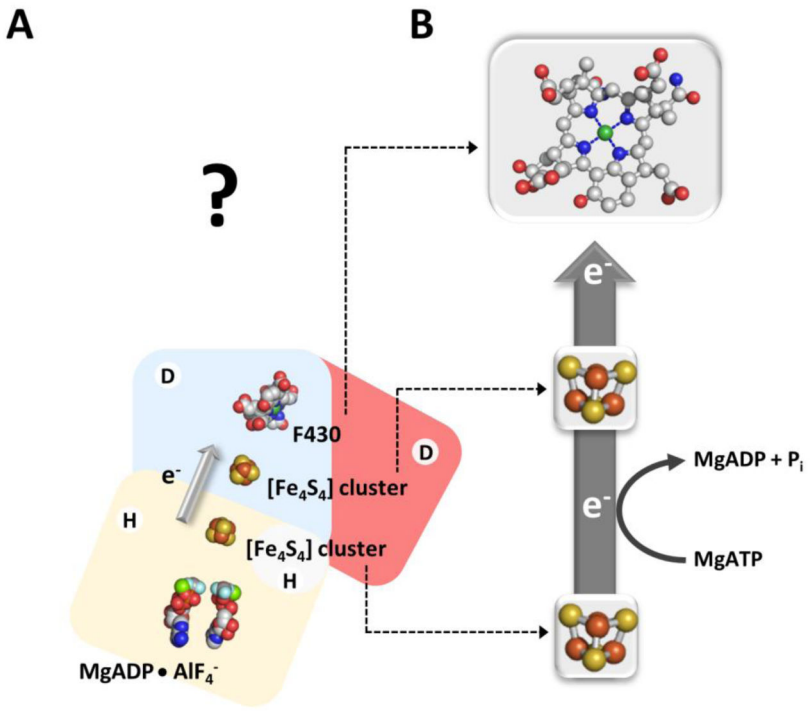

Fig. 5.

(A) Schematic presentation (transparent) of the hypothetical structural layout of the MgADP•AlF_4^--stabilized NflH/NflD complex. MgADP•AlF_4^-, [Fe_4S_4] clusters and cofactor F430 are shown as space-filling models. The two subunits of NflH (labeled as H) are colored gray and light wheat, respectively, and the two subunits of NflD (labeled as D) are colored red and light blue, respectively. **(B)** Components involved in the proposed electron transfer during catalysis. All clusters and cofactor F430 are shown as ball-and-stick models. Atoms are colored as follows: Fe, orange; S, yellow; V, dark gray; O, red; C, gray; N, blue; Mg, dark green; Al, light green; F, light blue.